Fusion Engineering and Design 85 (2010) 874–881

Contents lists available at ScienceDirect

Fusion Engineering and Design

journal homepage: www.elsevier.com/locate/fusengdes

Experiments with liquid metal walls: Status of the lithium tokamak experiment

Robert Kaita[a,*], Laura Berzak[a], Dennis Boyle[a], Timothy Gray[a], Erik Granstedt[a], Gregory Hammett[a], Craig M. Jacobson[a], Andrew Jones[a], Thomas Kozub[a], Henry Kugel[a], Benoit Leblanc[a], Nicholas Logan[a], Matthew Lucia[a], Daniel Lundberg[a], Richard Majeski[a], Dennis Mansfield[a], Jonathan Menard[a], Jeffrey Spaleta[a], Trevor Strickler[a], John Timberlake[a], Jongsoo Yoo[a], L. Zakharov[a], Rajesh Maingi[b], Vlad Soukhanovskii[c], Kevin Tritz[d], Sophia Gershman[e]

[a] Princeton Plasma Physics Laboratory, Princeton, NJ, USA
[b] Oak Ridge National Laboratory, Oak Ridge, TN, USA
[c] Lawrence Livermore National Laboratory, Livermore, CA, USA
[d] Johns Hopkins University, Baltimore, MD, USA
[e] Watchung Hills Regional High School, Warren, NJ, USA

ARTICLE INFO

Keywords:
Low-aspect ratio tokamaks
Lithium plasma-facing components
Low-recycling plasmas
Fusion reactor first walls
Plasma fueling

ABSTRACT

Liquid metal walls have been proposed to address the first wall challenge for fusion reactors. The lithium tokamak experiment (LTX) at the Princeton Plasma Physics Laboratory (PPPL) is the first magnetic confinement device to have liquid metal plasma-facing components (PFC's) that encloses virtually the entire plasma. In the current drive experiment-upgrade (CDX-U), a predecessor to LTX at PPPL, the highest improvement in energy confinement ever observed in ohmically heated tokamak plasmas was achieved with a toroidal liquid lithium limiter. The LTX extends this liquid lithium PFC by using a conducting conformal shell that almost completely surrounds the plasma. By heating the shell, a lithium coating on the plasma-facing side can be kept liquefied. A consequence of the low-recycling conditions from liquid lithium walls is the need for efficient plasma fueling. For this purpose, a molecular cluster injector is being developed. Future plans include the installation of a neutral beam for core plasma fueling, and also ion temperature measurements using charge-exchange recombination spectroscopy (CHERS). Low edge recycling is also predicted to reduce temperature gradients that drive drift wave turbulence. Gyrokinetic simulations are in progress to calculate fluctuation levels and transport for LTX plasmas, and new fluctuation diagnostics are under development to test these predictions.

1. Introduction

The challenges imposed by the fusion reactor environment are well known. Because of the susceptibility of solid materials to damage under large heat loads and high energetic particle fluxes, liquid metals have been proposed as a possible first wall alternative [1]. Experiments with a large liquid lithium free surface were performed for the first time in a tokamak on the current drive experiment-upgrade (CDX-U) at the Princeton Plasma Physics Laboratory (PPPL).

A 2000 cm^2 toroidal liquid lithium limiter was installed in the bottom of the CDX-U vacuum vessel. Efficient convective heat dissipation was demonstrated with an electron beam that simulated power loads of up to 60 MW/m^2 on the lithium surface [2]. More recent electron beam work on a separate test facility indicated that thermoelectric currents were responsible for the convection observed in the liquid lithium [3].

Equally important for reactor applications is the effect a liquid lithium wall would have on plasma performance [4]. The concept could be tested in a device with liquid lithium wall coatings, which are anticipated to reduce recycling to the vicinity of ~20%. With low recycling, edge fueling is no longer the dominant particle source for the plasma. Under these conditions, discharges with core fueling are expected to have edge electron temperatures that rise, and internal temperature gradients that are greatly reduced. Lowering the internal temperature gradient should substantially lower or eliminate the major free energy source for temperature gradient-driven turbulence, which is believed to be the principal cause of anomalous electron and ion transport. For this reason, liquid lithium walls should lead to a significant improvement in tokamak electron confinement.

These predictions were initially investigated in CDX-U. With the toroidal liquid lithium limiter and solid lithium wall coatings from evaporation between shots, the recycling in CDX-U was reduced to

* Corresponding author. Tel.: +1 6092433275; fax: +1 6092432148.
E-mail address: kaita@pppl.gov (R. Kaita).

0920-3796/$ – see front matter © 2010 Elsevier B.V. All rights reserved.
doi:10.1016/j.fusengdes.2010.04.005

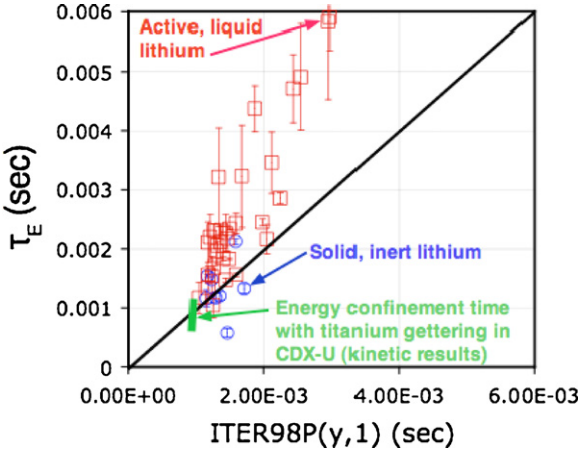

Fig. 1. Comparison of measured confinement times on CDX-U with predictions from ITER98p(y,1) scaling.

about ~50%. This is the lowest level of recycling level ever observed in a magnetic confinement device, and it was associated with a large increase in the energy confinement time.

In the presence of a liquid lithium limiter and newly deposited lithium wall coatings, the energy confinement time increased by up to a factor eight over comparable discharges without such lithium surface conditions. This improvement in energy confinement significantly exceeded previous results with titanium gettering and boronization. These techniques had comparable effects on CDX-U, which remains the only magnetic confinement device where they have been directly compared with the effects of lithium.

The CDX-U results demonstrated the largest relative increase in energy confinement ever recorded for ohmic plasmas in any tokamak [5]. Furthermore, the highest confinement times of 5–6 ms are greater than the best values achieved in the START experiment. The physical dimensions and toroidal field in START were comparable to CDX-U. The START plasmas, however, were highly shaped and elongated divertor discharges. They were neutral-beam heated H-mode plasmas, and at currents of a few hundred kA, they exceeded CDX-U values by a factor of four.

The START confinement follows the ITER 98P(y,1) scaling shown in Fig. 1. The CDX-U results for plasmas in the presence of active lithium walls exceeded its expected values by a factor of 4–6. Because the ITER98p(y,1) scaling has a power dependence of $\sim P^{-0.69}$, the confinement appears to be due entirely to the observed reduction in the loop voltage, and hence the ohmic input power (Fig. 2). These findings are discussed in more detail elsewhere [2,5].

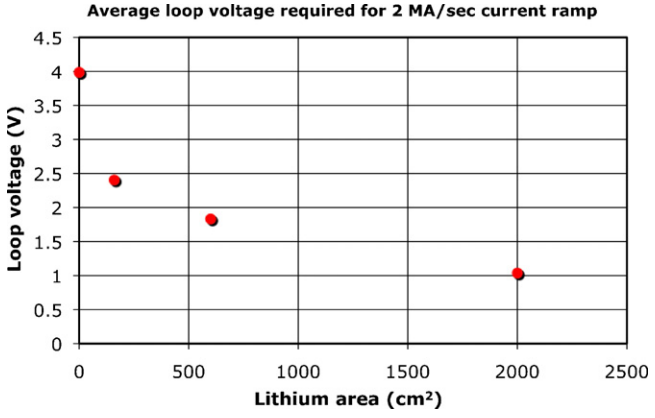

Fig. 2. Dependence of loop voltage for current ramp of 2 MA/s on active lithium surface area in CDX-U.

Table 1
LTX parameters.

Parameter	Value
Major radius	0.4 m
Minor radius	0.26 m
Toroidal field	0.34 T
Plasma current	400 kA
Current flattop	<250 ms
Ohmic flux	160 mV s

The lithium tokamak experiment (LTX) was motivated by the CDX-U results. As the first magnetic confinement device in the world to have lithium as a liquid metal plasma-facing component (PFC) that almost completely surround the plasma, LTX replaces the CDX-U limiter tray with a conducting conformal shell. By heating the shell above the lithium melting point, a lithium coating on the plasma-facing side can be kept in its liquid state. The basic design features of the LTX are described in Section 2.

One of the consequences of the low-recycling conditions from liquid lithium walls is the need for efficient plasma fueling. In addition to the supersonic gas injector used on CDX-U, a molecular cluster injector (MCI) is being developed. Future plans include the installation of a neutral beam for core plasma fueling, and also ion temperature measurements using charge-exchange recombination spectroscopy (CHERS). The MCI is described in Section 3, and the diagnostics for LTX are discussed in Section 4.

Analysis of the CDX-U results suggests that in its ohmic plasmas, the confinement increase could only be in the electron channel. This indicates suppression of anomalous electron transport due to drift wave turbulence, and low edge recycling is predicted to reduce temperature gradients that are its driving mechanism. Gyrokinetic simulations are in progress to calculate such effects for LTX plasmas, and preliminary results from the modeling are described in Section 5. A summary of recent activities on LTX, including the status of magnetics measurements and power supply upgrades, is provided in Section 6.

2. Engineering description of LTX

The LTX device is a modest-sized low aspect ratio tokamak. Its parameters are summarized in Table 1. The CAD drawing in Fig. 3 shows the key features of LTX. The salient component inside the vacuum vessel is a heated conducting shell, which is designed to enclose 90% of the last closed flux surface of the plasma. The plasma-facing surface of the shell will be coated with a thin liquid lithium film. This will be evaporatively deposited, and retained by simple wetting and surface tension up to a thickness of ~100 μm.

The shell consists of four isolated sections, each consisting of 1.5 mm thick 304 L stainless steel explosively bonded to 1 cm thick OFHC copper. Copper was chosen because its good heat conductivity provides a uniform temperature distribution, and the stainless steel liner prevents it from reacting with the liquid lithium. Commercial resistive cable heaters are mounted on the surface facing away from the plasma (Fig. 4), and they are used to maintain a temperature of up to 500–600 °C. These heaters have cold sections that are fed through vacuum fittings, so that all electrical connections can be made outside of the vacuum vessel. The shell has been raised to a temperature of 200 °C, or above the melting point of lithium. Under these conditions, the temperature of the outer Inconel surface of the center stack was kept to about 2 °C, while the vacuum vessel remained below 50 °C with only air cooling.

The upper and lower shell sections are separated to allow toroidally continuous diagnostic access in addition to an electrical break (Fig. 5). Each of these sections, in turn, has two segments that eliminate toroidal electrical paths, and enable poloidal views of the plasma. The shell segments are supported by legs that extend

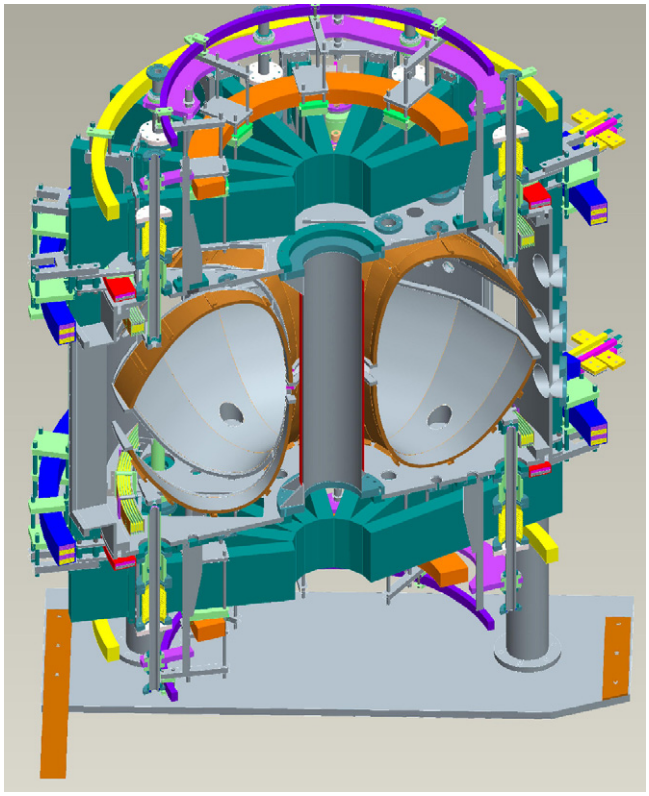

Fig. 3. LTX drawing showing field coil and internal heated conducting shell.

through the upper and lower vessel flanges through a vacuum electrical break and a formed bellows. These can be seen in the photograph of the top of LTX in Fig. 6. The electrical breaks are the light bands below the bellows. The shell segment-mounting scheme, together with electrical breaks on the heater feedthroughs, provides the isolation required for argon glow discharge cleaning of the inner shell surface. Additional details can be found in Ref. [6].

3. Fueling with molecular cluster injector

In addition to the removal of the edge localized particle source, operation with low global particle recycling should lead to high edge plasma temperatures. This is because in a tokamak, the power

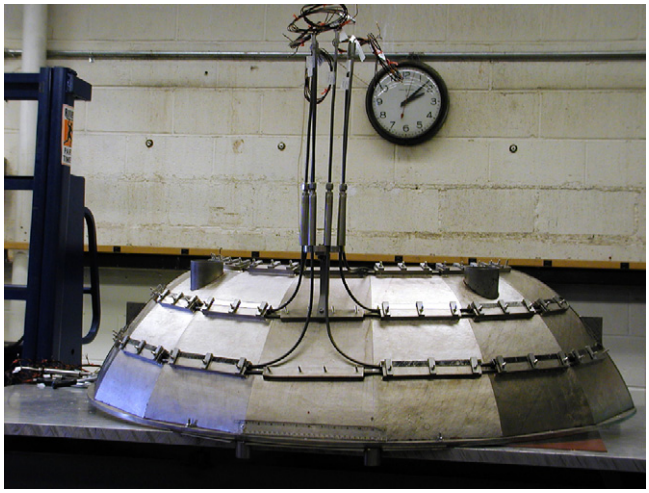

Fig. 4. Shell section with heaters on surface facing away from plasma.

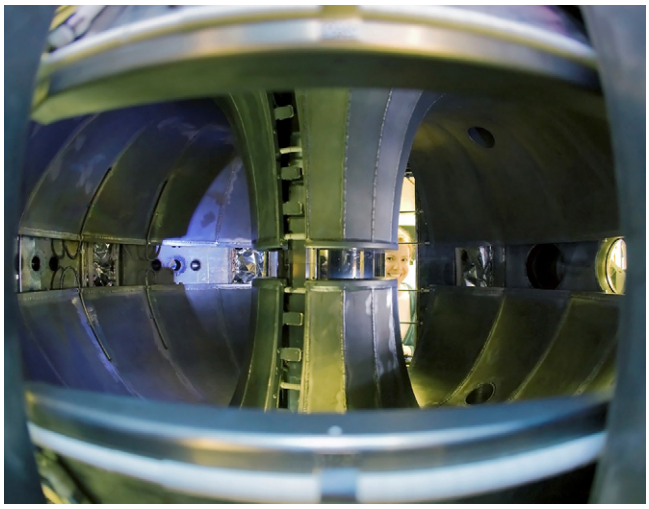

Fig. 5. Interior view of LTX through gap between upper and lower halves of heated conducting shell.

flow in the edge region is a convective process that involves the particle flux. In steady state, the total power flow across the edge must equal the power input to the core plasma. If the edge is the predominant source of particles, as is the case in a high recycling tokamak, the thermal energy per particle is small because a large edge particle population carries the power outflow.

With the same core input power in a low recycling tokamak, the edge particle population is much smaller. The power flow in the edge is then carried by far fewer particles. The energy per particle must then be higher under steady conditions, so this leads to larger edge temperatures in the presence of very low recycling walls.

Initially, fueling in LTX will use a combination of standard edge gas puffing and a supersonic gas injector (SGI) close-coupled to the plasma to improve fueling efficiency. The SGI was intended to improve penetration into the plasma volume beyond the mean free path of single neutral particles. The high density of the jet is expected to result in a shielding process where the outer particles block plasma electrons from colliding with the inner molecules of the jet. The limiting factor in the penetration of the molecules is then the pressure balance between the plasma and the jet.

Improved fueling efficiency has been demonstrated with SGI, for example, on NSTX. However, it still appears to be largely an

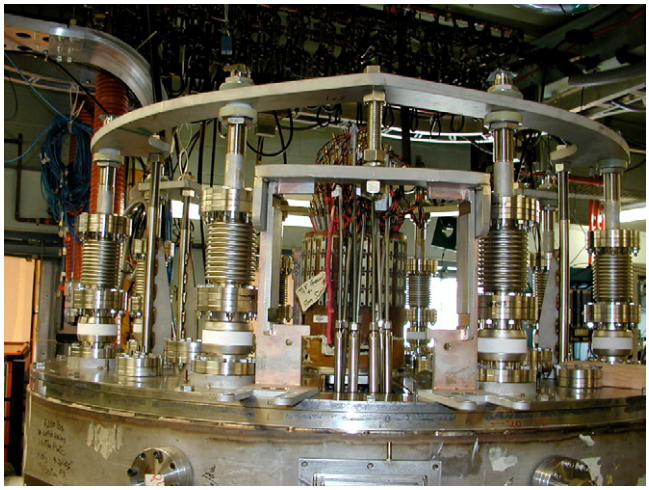

Fig. 6. Shell mounts above LTX vacuum vessel.

edge-localized particle source. Previous work indicates that the Franck-Condon energy of dissociating molecules is so large that it dominates any shielding effect that the jet density might have to provide more efficient fueling [7]. This has motivated the investigation of a different approach to improve fueling efficiency through better particle penetration.

An MCI system is under development for LTX. The MCI concept has been used in past fusion devices like the HL-2A machine in China. There, an existing supersonic molecular beam injection (SMBI) system was modified by cooling it to cryogenic temperatures [8] The SMBI is similar to the SGI described above. Compared to the room-temperature SMBI, the increase in the plasma density from the cryogenic jet was twice as large, and occurred at a deeper radius.

On LTX, the MCI uses a Parker Series 99 fast solenoid gas valve with a 0.02-in. orifice. This is capable of creating pulses as fast as 500 μs. The fueling pulses on LTX will be typically a few milliseconds in length. A Laval nozzle, similar to the type used in the SGI, is connected to the output of the valve, to collimate the flow into a jet and provide additional cooling due to the expansion in the flow. Unlike the SGI, which needs the valve to be closely coupled to the plasma edge so that the jet pressure is sufficient to provide penetration, the cluster injection forms clusters whose penetration length is primarily determined by their size, not the jet pressure and velocity.

It should be noted that some molecular cluster formation was anticipated with the SGI, since the gas was expected to cool as it entered the supersonic flow region of the Laval nozzle. This did not occur, however, since the temperature of the input gas may have been too high, and it could also have been warmed by the uncooled nozzle wall. This is mitigated on the approach for LTX MCI by cooling both cluster injector nozzle and the body of the solenoid valve.

The MCI for LTX is cooled with liquid nitrogen. Operating at about 80 K improves the cluster formation efficiency because of its dependence on the pre-expansion temperature ($T^{-2.29}$). As the gas cools, it forms clusters of molecules, each consisting of about the 1000–10,000 particles. The cluster formation depends on directly on the nozzle diameter and the pressure at its input, and inversely with the temperature there [9].

Fig. 7 shows the gas valve for the LTX MCI, with a cryogenic cooling blanket and copper cooling tubes attached to the valve body. Liquid nitrogen or pressurized nitrogen gas is forced through the tubes to cool the assembly. Cooling the valve in turn cools the gas in the valve body. Additional cooling occurs as the gas expands through the nozzle into vacuum.

The jet widths for the MCI were measured using a pressure transducer that was move across the output of the nozzle. The measurements with and without cryogenic cooling are compared at three different locations relative to the nozzle in Figs. 8 and 9, respectively. Both profiles show a decrease in the peaking with increasing distance from the nozzle.

The salient observation, however, is the substantially higher signals overall with the cooled nozzle. The data do not allow a direct comparison of the output pressure with the uncooled nozzle, since the time response of the transducer differs in the two cases. It is much slower with the cooled nozzle, apparently due to the recovery time of the valve membrane from deformation at cryogenic temperatures.

Nonetheless, there is enough of a difference to suggest cluster formation when the nozzle is cooled. This is supported by preliminary measurements of the visible emission as an electron beam crosses the output jet, and further characterization of the MCI is in progress. Different nozzle designs are also going to be tested to determine their effects on cluster formation efficiency.

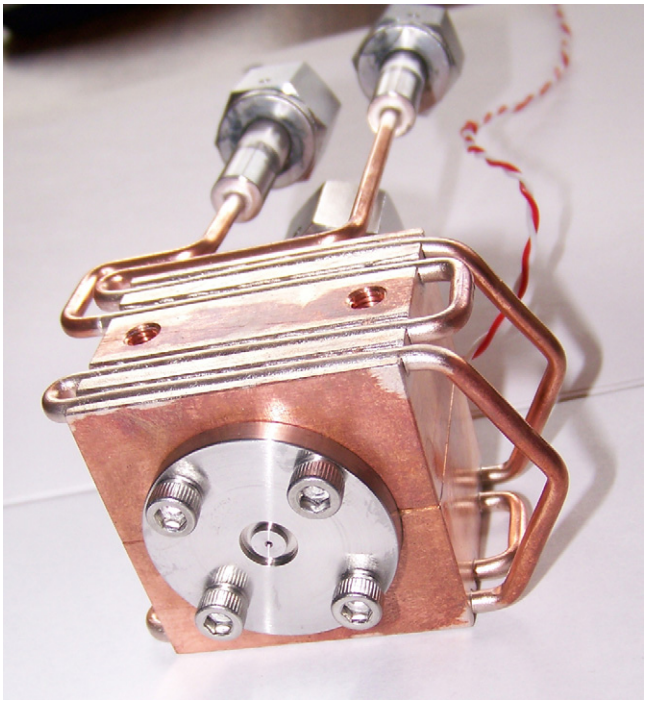

Fig. 7. Gas valve for MCI with cooling lines.

4. Plasma diagnostics

The dramatic effects of liquid lithium PFC's on the energy confinement in CDX-U were deduced from diamagnetic loop data. Measurements of electron temperature and density profiles are critical, however, for the detailed testing of the predictions for low recycling walls on plasma performance. For example, core electron temperature gradients are a significant source of free energy for instability drive. Their reduction or elimination is assumed to be responsible for the decrease in anomalous electron transport in the presence of liquid lithium walls, and this can only be directly verified with temperature profile data.

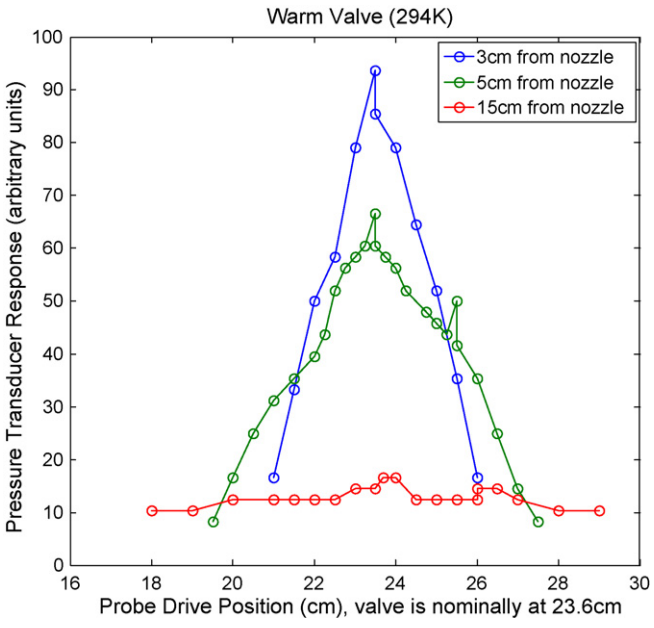

Fig. 8. Exit jet profiles for uncooled MCI.

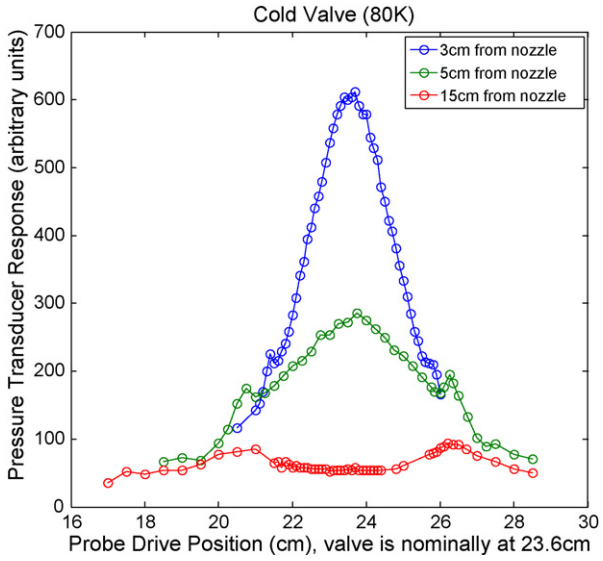

Fig. 9. Exit jet profiles for cooled MCI.

A Thomson scattering (TS) diagnostic is in the final stages of preparation for LTX. While a TS system was available on CDX-U prior to the liquid lithium PFC experiments, its usefulness was limited by low laser power and poor light transmission through the fiber optics between the collecting lens and the spectrometer. For LTX, the ruby laser power has been increased by about an order of magnitude to about 15 J. The TS system is presently configured to measure 12–16 spatial points across the core region of the plasma. There are plans to add five additional channels to observe the edge region with high spatial resolution (~1–2 mm). Fig. 10 shows some of the TS components installed on LTX. The edge of the laser enclosure is on the left. The horizontal flight tube in the middle of picture provides the beam path to the vacuum vessel on the right. Collection optics are supported by the structure in the center of the figure.

Neutral beam injection is also being planned on LTX. Funding has been received to prepare the machine room for a diagnostic neutral beam (DNB) that was initially developed for the National Compact Stellarator Experiment (NCSX). The DNB was designed for a one second, 5 A pulse at 40 keV. For LTX the acceleration grids will be modified for operation in the 15–20 keV range. This will optimize beam deposition, and still provide enough power for effective ion heating in LTX.

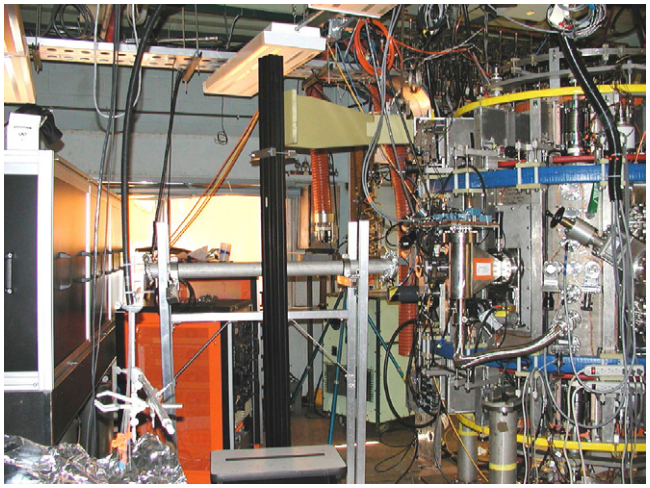

Fig. 10. Thomson scattering diagnostic on LTX.

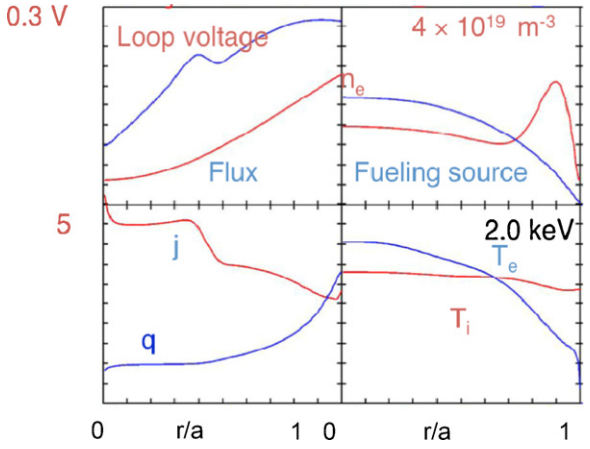

Fig. 11. Plasma profiles from ASTRA simulation for LTX.

The low loop voltage in plasmas with lithium PFC's means that the total ohmic input power is small. Loop voltage values of about 0.4 V were needed to maintain plasma currents in the 100 kA range in CDX-U. The loop voltages for LTX are expected to be in the range of 0.2–0.3 V, at densities where the electron-ion coupling is low. Under these conditions, the 90–100 kW available from the lower energy NCSX DNB should increase the central ion temperature to $T_i \sim 1$ keV. These predictions are based on simulations with the ASTRA transport code [10], which are shown in Fig. 11 [11].

The DNB will also enable core ion temperature measurements, with lithium as the impurity for CHERS. This technique has been successfully demonstrated on NSTX [12]. In addition, the DNB can be used for beam emission spectroscopy (BES) to obtain spatially localized measurements of core density fluctuations. These results can be compared with theoretical predictions for plasma turbulence, which are described in the next section.

5. Turbulence modeling

In the theoretical limit of zero recycling from the wall, the edge plasma has no interaction with the wall. In this region, the core temperature can then be equaled or even exceeded. Under these conditions, instabilities driven by temperature gradients, i.e., ITG, ETG, and micro-tearing modes are suppressed. Other transport mechanisms still remain, include parallel transport along stochastic field lines, TEM drift-wave turbulence driven by the density gradient, and neoclassical collisional transport.

To see what kind of instability suppression might be responsible for the confinement improvement in the CDX-U liquid lithium PFC plasmas, a so-called reference transport model (RTM) was implemented in the ASTRA-ESC transport-equilibrium and stability codes [10,13].

The RTM assumes that all transport was taking place at the ion neoclassical rate. The energy loss rate due to recycling from the walls was set to zero, and the external fueling was varied to match the plasma β deduced from CDX-U measurements. The model then gave values that approximated the experimental internal inductance, the loop voltage, the global energy confinement time, the central plasma density, and the central electron temperature inferred from Spitzer resistivity.

To simulate the effects of ITG and TEM drift wave turbulence, transport coefficients from the GLF23 model [14] were added to the RTM calculations. The results were very similar, so these effects do not appear to contribute to the transport. The modeling for CDX-U is not a definitive test of the RTM, however, since diagnostics for critical plasma parameters were unavailable. There were no direct electron and ion temperature profile measurements and fluctua-

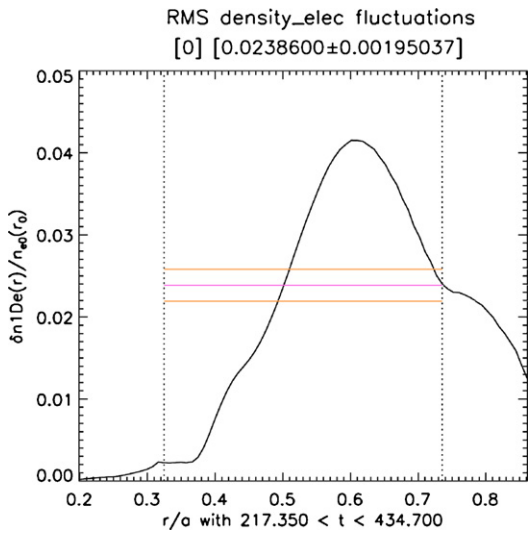

Fig. 12. Dependence of calculated density fluctuation amplitudes on normalized LTX minor radius.

tion data. As mentioned in the previous section, LTX will have the instrumentation to provide such information.

In anticipation of the LTX experiments, simulations are being performed to estimate density fluctuation levels. They use the GYRO program, which is a continuum global gyrokinetic code for investigating the effects of drift wave turbulence and other mechanisms that affect tokamak transport [15].

Preliminary density fluctuation amplitudes from nonlinear simulations, based on the profiles generated with ASTRA-ESC for LTX, are shown as a function of normalized minor radius in Fig. 12. At these levels, they should be observable with the BES diagnostic. The expected fluctuations in the plasma potential are depicted as poloidal contours in Fig. 13.

6. Recent LTX activities

Tokamak plasmas were difficult to obtain in LTX with the same field coil programming used on CDX-U. This is believed to be due to the effect of the new 1 cm thick conformal copper shell. Measurements with an extensive set of magnetic sensors on LTX [16] support this conclusion. Field coils were pulsed without plasmas, and the sensor responses were compared with model predictions with and without the shell included.

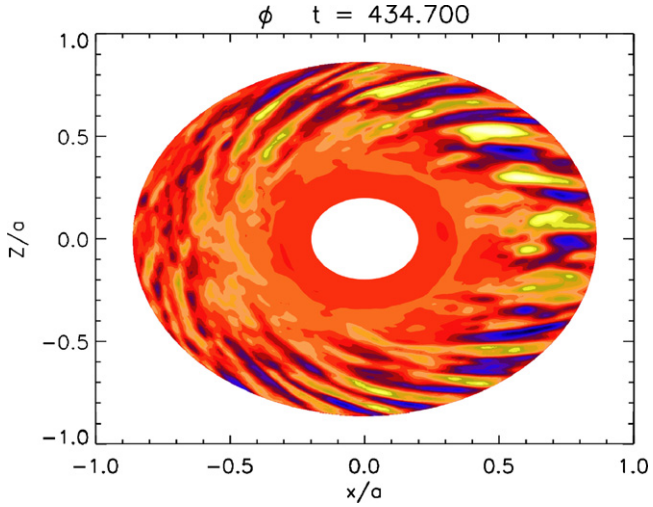

Fig. 13. Contours of simulated plasma potential fluctuations.

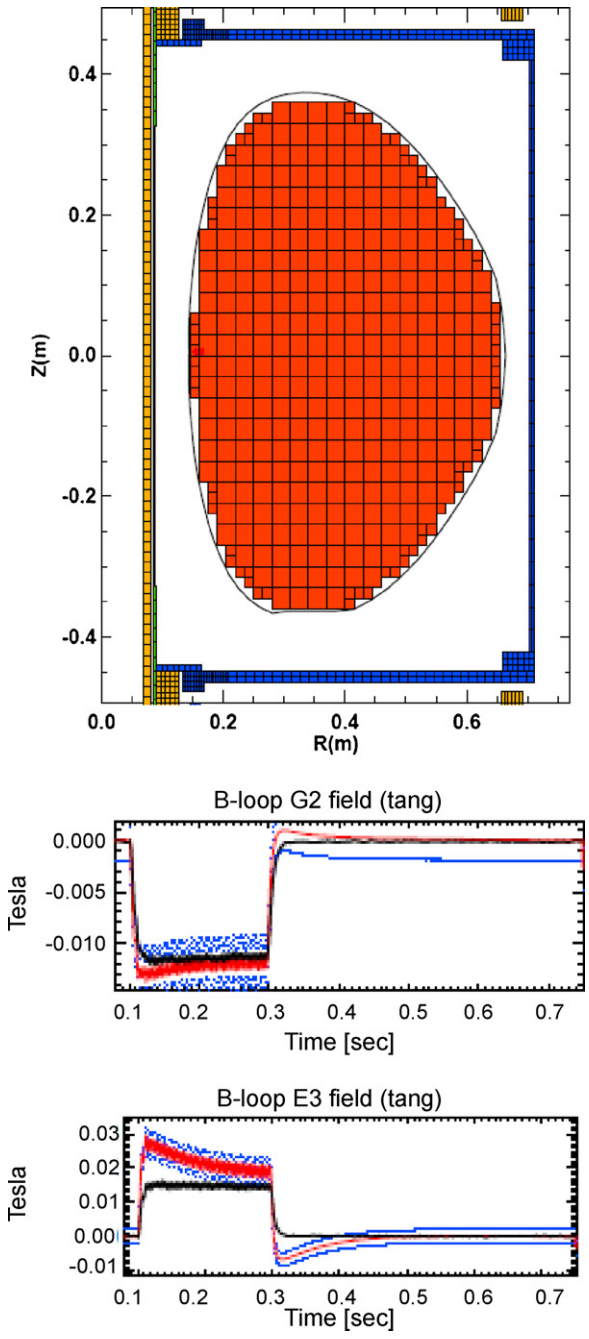

Fig. 14. Comparison of measured magnetic sensor signal with simulation using two-dimensional model. Upper plot shows LTX cross-section for model without shell. Middle and lower plots compare calculated and measured signals from inboard and exterior sensors, respectively.

The results are shown in Figs. 14 and 15. The upper plots show the LTX cross sections used in the LRDFIT program. This is a Grad–Shafranov equilibrium reconstruction code, where the contributions from currents induced in conducting structures can be included in the signals magnetic sensors are expected to measure.

Without the LTX shell, the calculated signal falls within the range of data from a sensor in the gap between the upper and lower shell halves (middle plot in Fig. 14). For a sensor on the outer shell surface, and thus separated from the plasma chamber by the thickness of the copper, the agreement is poorer (lower plot). The calculated signal is more square, and does not follow the rapid rise and slower decay of the data.

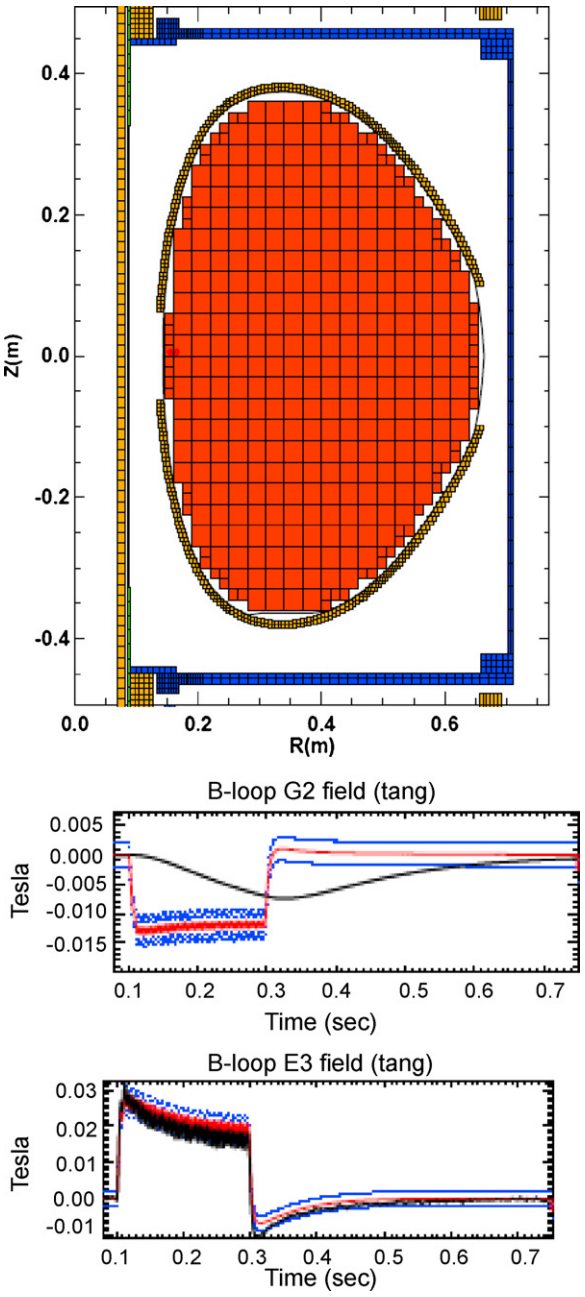

Fig. 15. Comparison of measured magnetic sensor signal with simulation using two-dimensional model. Upper plot shows LTX cross-section for model with shell. Middle and lower plots compare calculated and measured signals from inboard and exterior sensors, respectively.

The situation reverses when the shell is introduced in the calculation (Fig. 15). The calculated signal follows the time dependence of the data for the sensor on outer shell surface (lower plot), but exhibits a much slower rise and decay than the sensor in the shell gap detects.

This discrepancy is attributable to the fact that LRDFIT is a two-dimensional program. Three-dimensional calculations are in progress for more accurate modeling of the LTX geometry. Data for each magnetic sensor are first obtained by pulsing the field coils individually. They are then used by the Cbc2e code developed by L. Zakharov to determine response functions that reflect the actual vessel eddy currents. This results in calibrations for sensor signals that can be used in a Grad–Shafranov solver (ESC), without any assumptions about axisymmetry.

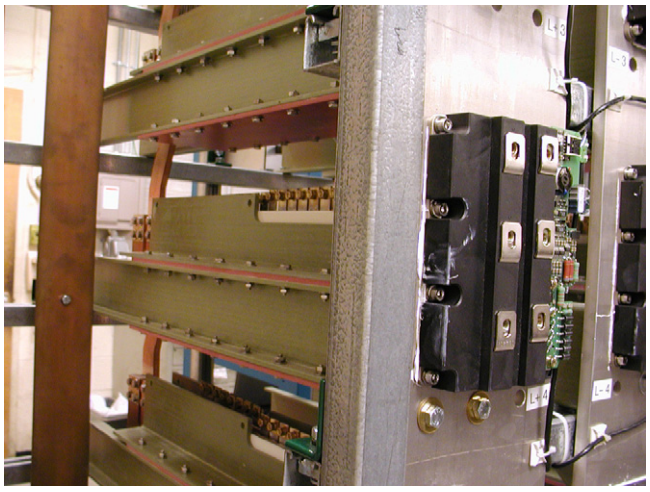

Fig. 16. IGBT and compensating transformers for new LTX OH supply.

In spite of its limitations, the two-dimensional analysis did confirm that shell effects, which were not present in CDX-U, had to be considered in developing the new plasma startup scenarios required for LTX. The field coil programming was adjusted until the magnetic sensor signals were consistent with the null formation required for breakdown.

There were also indications that the filament used for discharge initiation on CDX-U was not adequate for LTX. This motivated the installation of a 1 kW pulsed electron cyclotron heating (ECH) system at 5.6 GHz for more efficient preionization. With ECH plasma initiation and appropriate field coil programming, tokamak discharges are routinely achievable on LTX.

Lithium wall experiments are about to begin, in parallel with the final testing and commissioning of the first phase of a new OH supply. It has the unique feature of using transformer coupling of the individual, parallel insulated-gate bipolar transistors (IGBT's) switches. Fig. 16 shows one of the IGBT's, with some of the transformers mounted behind it.

The combination of IGBT's with compensating transformers allows staggered firing of the IGBT's in each arm of the H-bridge power supply. It is the first time that such an arrangement has been used in a high current, high power system.

The capacitor bank for this initial implementation, which will have 330 kJ of stored energy, is shown in Fig. 17. Funding has recently been received for the second phase, which will raise the

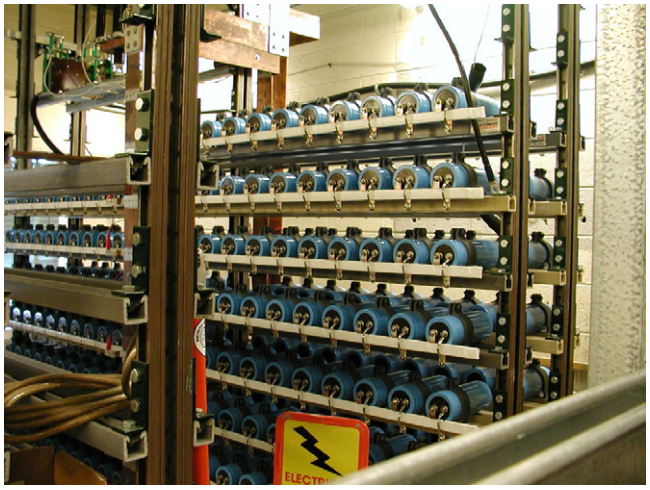

Fig. 17. Capacitor bank for first phase of new LTX OH supply.

stored energy to 1.3 MJ. When completed, plasma currents up to 400 kA for 250 ms will be possible.

Acknowledgement

Work supported by US Department of Energy Contracts DE-AC02-09CH11466, DE-AC04-94AL85000, DE-AC52-07NA27344, and DE-AC05-00OR22725.

References

[1] M. Abdou, A. Ying, N. Morley, K. Gulec, S. Smolentzev, M. Kotschenreuther, et al., Fusion Eng. Des. 54 (2001) 181.
[2] R. Kaita, R. Majeski, T. Gray, H. Kugel, D. Mansfield, J. Spaleta, et al., Phys. Plasmas 14 (2007) 056111.
[3] M. Jaworski, N. Morley, D. Ruzic, J. Nucl. Mater. 390–391 (2009) 1055.
[4] S. Krasheninnikov, L. Zakharov, G.V. Pereverzev, Phys. Plasmas 10 (2003) 1678.
[5] R. Majeski, R. Doerner, T. Gray, R. Kaita, R. Maingi, D. Mansfield, et al., Phys. Rev. Lett. 97 (2006) 075002.
[6] R. Majeski, H. Kugel, R. Kaita, Fusion Eng. Des. (2009), doi:10.1016/j.fusengdes.2010.03.020.
[7] D. Lundberg, R. Kaita, T. Kozub, R. Majeski, V. Soukhanovskii, in: 49th Annual Meeting of the Division of Plasma Physics TP8.00100, Bull. Am. Phys. Soc. 52 (2007).
[8] L. Yao, B. Feng, C. Chen, Z. Shi, B. Yuan, Y. Zhou, Nucl. Fusion 47 (2007) 1399.
[9] O. Hagena, Rev. Sci. Instrum. 63 (1992) 4.
[10] G. Pereverzev and P. Yushmanov, ASTRA: an automatic system for transport analysis in a tokamak, Rep. IPP 5/42, Max-Planck-Institut fur Plasma-physik, Garching (1991).
[11] M. Bell, H. Kugel, R. Kaita, L. Zakharov, H. Schneider, B. LeBlanc, et al., Plasma Phys. Control. Fusion 51 (2009) 124054.
[12] R. Majeski, L. Berzak, T. Gray, R. Kaita, T. Kozub, F. Levinton, et al., Nucl. Fusion 49 (2009) 055014.
[13] L.E. Zakharov, A. Pletzer, Phys. Plasmas 6 (1999) 4693.
[14] R. Waltz, G. Kerbel, J. Milovich, G. Hammett, Phys. Plasmas 4 (1997) 2482.
[15] J. Candy, R. Waltz, J. Comput. Phys. 186 (2003) 545.
[16] L. Berzak, R. Kaita, T. Kozub, R. Majeski, L. Zakharov, Rev. Sci. Instrum. 79 (2008), 10F116.